Superfluid density of the $\pm$s-wave state for the iron-based superconductors

YUNKYU BANG[1,2]

[1] *Department of Physics, Chonnam National University, Kwangju 500-757, Korea*
[2] *Asia Pacific Center for Theoretical Physics, Pohang 790-784, Korea*

arXiv:0902.1020v3 [cond-mat.supr-con] 5 May 2009

PACS 74.20.-z – Theories and models of superconducting state
PACS 74.20.Rp – Pairing symmetries (other than s-wave)
PACS 74.25.Nf – Response to electromagnetic fields

Abstract. - We study the superfluid density of the $\pm$s-wave state of the minimal two band model for the Fe-based superconductors and its evolution with impurity concentration. We show that the impurity scattering of the strong coupling limit induces the selfenergy of a generic form $Im\Sigma_{imp}(\omega) \approx i\gamma + i\beta\omega$ beyond a critical impurity concentration $\Gamma_{imp} > \Gamma_{crit}$. This form of $Im\Sigma_{imp}(\omega)$ causes the temperature dependence of the superfluid density $[\rho_s(T) - \rho_s(0)] \approx -\gamma T^2 - \beta T^3$. Combining with the full gap behavior of $\rho_s(T)$ for lower impurity concentration $\Gamma_{imp} < \Gamma_{crit}$, the $\pm$s-wave state produces a continuous evolution of $\Delta\lambda(T)$: exponentially flat $\rightarrow T^3 \rightarrow T^2$ with increasing impurity concentration that is consistent with the measurements of the Fe pnictide superconductors such as *M*-1111 (*M*=La,Nd,Sm,Pr) and Ba-122 with various dopings, except LaFePO which shows $\Delta\lambda(T) \propto T^{1.2}$ at low temperatures by recent experiment. Our results also demonstrate that the density of states (DOS) measured by thermodynamic properties and the DOS measured by transport properties can in general be different.

Introduction. – The recent discovery of Fe-based superconducting compounds [1–3], has greatly spurred the research of unconventional superconductors. With a discovery of new superconducting (SC) material, the most impelling question is to determine the SC gap symmetry. However, despite intensive experimental efforts, the pairing symmetry of this new class of SC materials is not completely settled.

Tunneling spectroscopy of Ref. [4, 5], photoemission spectroscopy of Ref. [6], and NMR nuclear-spin-lattice relaxation rate measurements [7–11] seem to indicate a nodal superconductors (SCs). On the other hand, tunneling spectroscopy of Ref. [12], angle resolved photoemission spectroscopy (ARPES) measurements of Ref. [13–15], specific heat measurement [16] all support a fully opened s-wave type gap. As to the penetration depth measurements, early measurements of *M*-1111 (*M*=Pr, Nd, Sm) [17–19], and (Ba,K)Fe_2As_2 [20] showed an exponentially flat behavior at low temperatures supporting a s-wave type SC. However, recent reports of $Ba(Fe,Co)_2As_2$ [21, 22] shows a power law of $T^{2-2.5}$ and more recently measurement of LaFePO [23] shows a near T-linear temperature dependence.

On the theoretical side, it is almost agreed on that non-phononic fluctuation is the most probable pairing interaction and several theoretical proposals for the possible pairing symmetries of Fe pnictide SCs were put forward [24–28]. However, recent advance of theoretical studies by several groups [29–32] have provided convincing evidences that the $\pm$s-wave SC state is the most promising candidate for the true pairing state of Fe pnictide SCs. Therefore, we will consider only the $\pm$s-wave SC state in this paper.

Having s-wave gaps on each bands but with opposite signs, the $\pm$s-wave SC state would display standard features of a s-wave SC for various SC properties at its pure state, for example, the exponentially flat temperature dependence of the penetration depth, which is consistent with some of experiments [17–20]. Another hallmark of a s-wave pairing state is the Hebel-Slichter peak and exponential drop of the nuclear-spin-lattice relaxation rate $1/T_1$, which is absolutely inconsistent with the experimental reports of all Fe pnictide SC compounds [7–11]. It was quickly pointed out by several groups [28–32] that the opposite signs of the order parameters (OP) in the $\pm$s-wave SC state with a help of impurity scattering could reduce the Hebel-Slichter peak and also mitigate the exponential temperature dependence into a power law temperature dependence. In particular, the Ref. [29] showed the special importance of the strong coupling (unitary limit) impurity scattering in the $\pm$s-wave SC state. The source of strong coupling impurities is also naturally expected when there are detects or

vacancies on Fe sites, of which the concentration should be also very small (order of a few percents) unless the superconductivity itself is substantially or completely destructed.

To sketch briefly the previous work [29], impurity scattering of the strong coupling limit in the $\pm$s-wave SC state induces an impurity bound state inside the SC gap, which is however off-centered from zero energy due to the generic property of the $\pm$s-wave state, namely, *the unequal sizes of the s-wave OPs with opposite signs on different bands*. This impurity bound state drastically modifies the fully gapped DOS of the pure $\pm$s-wave state into a V-shaped DOS as in a d-wave SC. This V-shaped DOS is not only consistent with the DOS directly measured by tunneling spectroscopy [4, 5] but also conform with the isotropic gap measured by ARPES [13–15]; a d-wave state would give a V-shaped DOS but at the same time should show a strong anisotropy of the gap in the ARPES experiments. Furthermore, it provides a clear physical explanation for the origin of the $T^{\alpha}(\alpha \approx 3)$ power law of NMR $1/T_1$ measured for all Fe pnictide SCs [7–11]. This is an excellent theoretical success in that a noble interplay between the strong coupling impurities and the $\pm$s-wave gaps provides coherent resolutions to the several conflicting experimental observations with only one adjustable parameter, i.e., the impurity concentration.

In this paper, we extend the previous work [29] to study the superfluid density and penetration depth in order to complete the consistency test of the $\pm$s-wave state as the ground state of Fe pnictide SCs, except LaFePO [23]. The main results of this paper is that the temperature dependence of $\lambda(T)$ of the $\pm$s-wave state evolves systematically with increasing impurity concentration: from a exponentially flat behavior for pure sample to a T^3 behavior at a critical impurity concentration, and finally to a T^2 one beyond the critical impurity concentration. These temperature dependencies are in agreement with the data of *M*-1111 (*M*=Pr, Nd, Sm) [17–19] and (Ba,K)Fe_2As_2 [20] (exponentially flat), and Ba(Fe,Co)$_2As_2$ [21, 22] (power law $\propto T^{2-2.5}$). However, recent report of $\Delta\lambda(T) \propto T^{1.2}$ for LaFePO [23] is not compatible with our scenario. Possible explanation for this exception is that this compound may have a different pairing symmetry than the other Fe pnictide SC compounds [28]. We will not pursue this issue in the current paper.

Model and Formalism. – For the minimal two band model of the $\pm$s-wave pairing state, we assume two s-wave OPs Δ_h and Δ_e on the two representative bands of the Fe pnictide materials: one hole band around Γ point and one electron band around *M* point in the reduced Brillouin Zone. Δ_h and Δ_e have opposite signs and their magnitude are different in general. Impurity scattering will renormalize the energy (ω) and the OPs ($\Delta_{h,e}$) through the selfenergy corrections: normal selfenergy and anomalous selfenergy, respectively. These impurity induced selfenergies are calculated by the $\mathcal{T}$-matrix method [33, 34], suitably generalized for the $\pm$s-wave pairing model [29], as follows.

$$\tilde{\omega}_n = \omega_n + \Sigma_h^0(\omega_n) + \Sigma_e^0(\omega_n), \tag{1}$$

$$\tilde{\Delta}_{h,e} = \Delta_{h,e} + \Sigma_h^1(\omega_n) + \Sigma_e^1(\omega_n), \tag{2}$$

$$\Sigma_{h,e}^{0,1}(\omega_n) = \Gamma \cdot \mathcal{T}_{h,e}^{0,1}(\omega_n), \;\; \Gamma = \frac{n_{imp}}{\pi N_{tot}}, \tag{3}$$

where $\omega_n = T\pi(2n+1)$ is the Matsubara frequency, n_{imp} the impurity concentration, and $N_{tot} = N_h(0) + N_e(0)$ is the total DOS. The $\mathcal{T}$-matrices $\mathcal{T}^{0,1}$ are the Pauli matrices $\tau^{0,1}$ components in the Nambu space and defined as follows.

$$\mathcal{T}_a^i(\omega_n) = \frac{G_a^i(\omega_n)}{D} \quad (i = 0,1; \;\; a = h,e), \tag{4}$$

$$D = c^2 + [G_h^0 + G_e^0]^2 + [G_h^1 + G_e^1]^2, \tag{5}$$

$$G_a^0(\omega_n) = \frac{N_a}{N_{tot}} \left\langle \frac{\tilde{\omega}_n}{\sqrt{\tilde{\omega}_n^2 + \tilde{\Delta}_a^2(k)}} \right\rangle, \tag{6}$$

$$G_a^1(\omega_n) = \frac{N_a}{N_{tot}} \left\langle \frac{\tilde{\Delta}_a}{\sqrt{\tilde{\omega}_n^2 + \tilde{\Delta}_a^2(k)}} \right\rangle, \tag{7}$$

where $c = \cot\delta_0$ is a convenient measure of scattering strength, with $c = 0$ for the unitary limit and $c > 1$ for the Born limit scattering. $\langle \ldots \rangle$ denotes the Fermi surface average.

With the self-consistently calculated $\tilde{\omega}_n$ (Eq.(1)) and $\tilde{\Delta}_{h,e}$ (Eq.(2)), we can calculate all physical quantities of the model. For small amount of impurity concentration ($\Gamma/\Delta_e \ll 1$) of the strong scatterers ($c = 0$), which we believe the case of the relevant experiments, the T_c suppression is small [29] and the renormalization of the OPs $\tilde{\Delta}_{h,e}$ is also marginal. However, the renormalization of $\tilde{\omega}_n$ is strong even with a small amount of unitary scatterers and develops an off-centered impurity bound state inside the SC gap. This unusual low energy impurity band modifies the fully gapped DOS of the pure state into a V-shape DOS and becomes the origin of the power law ($\propto T^3$) of the NMR relaxation rate $1/T_1$ of Fe pnitide SCs [7–11]. In this paper, we study how this modified DOS of the $\pm$s-wave state with impurities affect the superfluid density and penetration depth.

Avoiding unnecessary repeat, we begin with showing previous calculations of the DOS $N_{tot}(\omega)$ and the corresponding normal selfenergy $Im\Sigma_{tot}^0(\omega) = Im\Sigma_h^0 + Im\Sigma_e^0$ for various impurity concentrations in Fig.1(a) and Fig.1(b). These results were calculated with the parameters $|\Delta_e|/|\Delta_h| = 2.5$ with $N_h(0)/N_e(0) = 2.6$, which were obtained with the realistic band structure parameters [29]. The physical results of the present paper, however, are independent of the specific choice of theses parameters. All energy scales are normalized by $|\Delta_e|$ in this paper. Fig.1(a) shows the total DOS with different impurity concentrations $\Gamma/\Delta_e = 0.0, 0.01, 0.04, 0.08$ of the unitary scatterer (c=0), and Fig.1(b) shows the corresponding impurity induced selfenergy $Im\Sigma_{tot}^0(\omega) = Im\Sigma_h^0 + Im\Sigma_e^0$.

Figure 1(a) shows systematic evolution of how the fully opened gap of pure state is filled with impurity states; the pattern of filling is very unusual and the $\Gamma/\Delta_e = 0.04$ case displays a perfect V-shape DOS down to zero energy similar to a pure d-wave SC DOS. The origin of this behavior is easily seen in Fig.1(b); the impurity bound state is never formed at zero energy but away from it because of the incomplete cancellation of $[G_h^1 + G_e^1]$ in D (Eq.(5)), the denominator of the $\mathcal{T}$-matrices

$\mathcal{T}^{0,1}$. Were the sizes of $N_h|\Delta_h|$ and $N_e|\Delta_e|$ equal, the FS averaged anomalous Green's functions $[G_h^1 + G_e^1]$ would vanish and then the impurity bound state would form at zero energy; this condition is intrinsically satisfied in the case of d-wave SC state. In generic ±s-wave state, therefore, *the full gap around* $\omega = 0$ *is protected* until this off-centered impurity band spills over to the zero energy with increasing impurity concentration. When it touches the zero energy limit, the ±s-gap state will thermodynamically behave like a pure d-wave SC, and this happens with the critical impurity concentration Γ_{crit} ($= 0.04\Delta_e$ for our specific model parameters). Increasing impurity concentration beyond Γ_{crit}, the DOS still keeps the V-shape but now $N_{tot}(\omega = 0)$ obtains a finite value (see the $\Gamma = 0.08\Delta_e$ case in Fig.1(a)).

Superfluid density and penetration depth. – With the above calculated $\tilde{\omega}_n$ and $\tilde{\Delta}_{h,e}$, we can study the temperature dependence of the superfluid density along the Fe-plane, with the following kernel.

$$K(T) = \frac{e^2}{c} \sum_{a=h,e} N_a 2\pi T \sum_n \left\langle v_{a\|}^2 \mathrm{Re} \frac{\tilde{\Delta}_a^2}{(\tilde{\omega}_n^2 + \tilde{\Delta}_a^2)^{3/2}} \right\rangle. \quad (8)$$

The above kernel is directly proportional to the superfluid density $\rho_s(T)$ and $1/\lambda_L^2(T)$ in the London limit. We use this formula for numerical calculations. Before we show the numerical results, we would like to gain analytic understanding about the temperature dependence of the superfluid density $\rho_s(T)$ of the ±s-wave state when the DOS is modified by impurity scattering as shown in Fig.1. To focus on the temperature dependence, we separate only the temperature dependent part from Eq.(8) as

$$\delta K(T) = -\frac{2e^2}{c} \sum_{a=h,e} N_a \left\langle v_{a\|}^2 \int_0^\infty d\omega f(\omega) \mathrm{Re} \frac{\tilde{\Delta}_a^2}{(\tilde{\omega}^2 - \tilde{\Delta}_a^2)^{3/2}} \right\rangle, \quad (9)$$

where $f(\omega)$ is Fermi-Dirac distribution function and $\tilde{\omega}$ and $\tilde{\Delta}_a(\omega)$ are the real frequency quantities obtained from $\tilde{\omega}_n$ and $\tilde{\Delta}_a(\omega_n)$ by analytic continuation ($\omega_n \to \omega + i\eta$). As explained before, for small impurity concentrations, $\tilde{\Delta}_a \approx \Delta_a$ and $\tilde{\Delta}_a$ doesn't develop any peculiar low energy structure, therefore we focus on the behavior of $\tilde{\omega} = \omega + \Sigma_{tot}^0(\omega)$ at low energies. As can be seen in Fig.1(b), for $\Gamma_{imp} > \Gamma_{crit}$ ($\Gamma_{crit} = 0.04\Delta_e$), we can approximate $\tilde{\omega} \approx a\omega + i\beta\omega + i\gamma...$ for low frequencies. Here γ is the typical impurity induced constant damping. Unusual part is the term $i\beta\omega$ which gives a linear-in-ω damping that is a unique feature of the ±s-gap state with impurity scattering of a strong coupling limit (unitary limit). With this form of $\tilde{\omega}$, we can extract the temperature dependence of $\delta K(T)$ using extended Sommerfeld expansion [35] at low temperatures. After straightforward calculation, we obtain the following result.

$$\delta K_a(T) \approx -\frac{2e^2 N_a v_{a\|}^2}{c} \times \left[\frac{\pi^2 \Delta_a^2 a\gamma}{4(\gamma^2 + \Delta_a^2)^{5/2}} T^2 + \frac{4\Delta_a^2 a\beta}{(\gamma^2 + \Delta_a^2)^{5/2}} \left(1 - \frac{5\gamma^2}{(\gamma^2 + \Delta_a^2)}\right) (1.35231)\, T^3 \right] ... \quad (10)$$

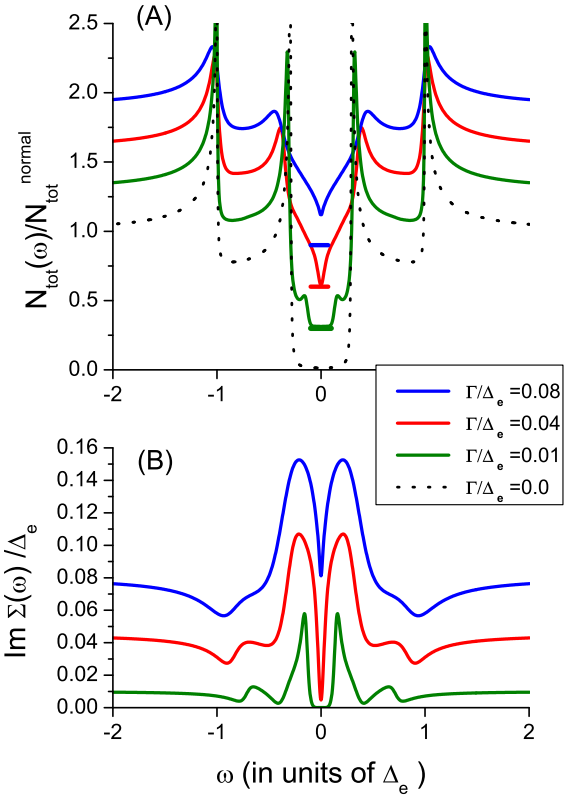

Fig. 1: (Color online) (a) Normalized DOS $N_{tot}(\omega)$ for different impurity concentrations, $\Gamma/\Delta_e = 0.0, 0.01, 0.04, 0.08$. Thin dotted line is of the pure state for comparison and other lines are offset for clarity (the zero baselines of the offset are marked by the narrow horizontal bars of the corresponding colors). (b) Impurity induced selfenergies $Im\Sigma_{tot}^0(\omega) = Im\Sigma_h^0 + Im\Sigma_e^0$ with the same parameters as in (a). These curves are not offset.

As expected from a power counting, the constant damping term γ produces T^2 decrease and the linear-in-ω damping term $\beta\omega$ produces T^3 decrease of superfluid density $\rho_s(T)$. The T^2 decrease of $\rho_s(T)$ due to a constant damping is the well known correction due to the strong coupling impurity scattering in the d-wave high-T_c cuprates [36]. What is unusual is the T^3 correction due to the linear-in-ω damping. This linear-in-ω damping is the unique feature of the ±s-wave SC with strong coupling (unitary limit) impurity scattering and it modifies otherwise fully opened DOS into a V-shape DOS. This V-shape DOS results in the same thermodynamic behaviors as in a d-wave SC such as in specific heat and NMR $1/T_1$ relaxation rate, etc. However, when transport property like the superfluidity density is calculated, specific vertex enters combined with the coherent factors and a naive picture based on the DOS fails.

With this result we have now a complete evolution of the temperature dependence of the superfluid density $\rho_s(T)$ for the ±s-wave SC with strong coupling impurities. For a clean sample ($\Gamma_{imp} < \Gamma_{crit}$), it will show an exponentially flat dependence at low temperatures. With increasing impurity concentration,

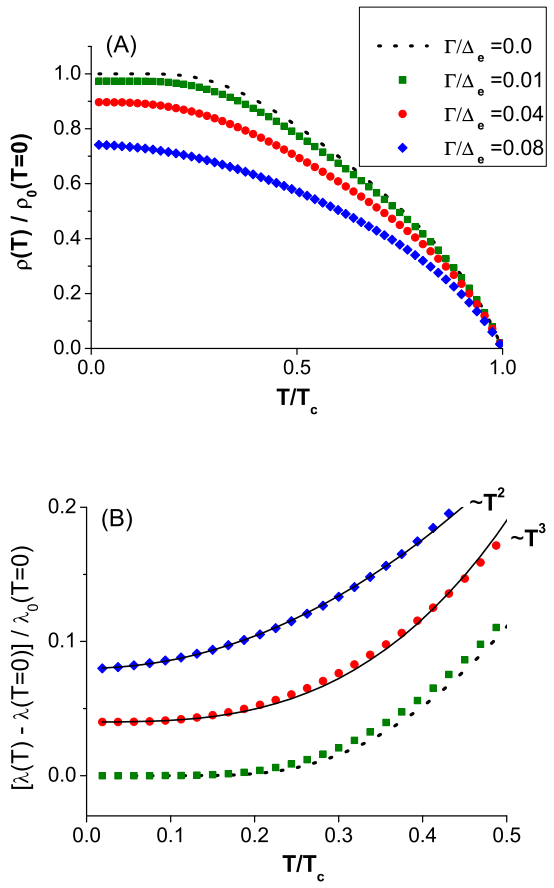

Fig. 2: (Color online) (a) Superfluid density $\rho_s(T)$ for different impurity concentrations, $\Gamma/\Delta_e = 0.0, 0.01, 0.04, 0.08$, normalized by $\rho_s^0(T=0)$ of the pure state. (b) Corresponding penetration depth $\Delta\lambda(T) = \lambda(T) - \lambda(T=0)$ normalized by $\lambda_0(T=0)$ of the pure state. The data for $\Gamma/\Delta_e = 0.04, 0.08$ are offset for clarity. The power law lines (sold black lines) of T^2 and T^3 are shown for comparison.

this flat temperature region shrinks. At the critical impurity concentration ($\Gamma_{imp} = \Gamma_{crit}$), it will display the T^3 behavior. And finally for $\Gamma_{imp} > \Gamma_{crit}$, the T^2 behavior will smoothly dominate over the T^3 dependence. Therefore, for a finite window of impurity concentrations of $\Gamma_{imp} > \Gamma_{crit}$, experiments would display a power law $\propto T^{\alpha}$ with $2 < \alpha < 3$. This evolution of temperature dependence with impurity concentration is consistent with the data of M-1111 (M=Pr, Nd, Sm) [17–19] (flat), (Ba,K)Fe_2As_2 [20] (flat), and Ba(Fe,Co)$_2As_2$ [21, 22] ($\propto T^{2-2.5}$), except for the data of LaFePO [23] ($\propto T^{1.2}$).

In Fig.2, we show the numerical results of $K(T)$ of Eq.(8) using the same parameters as in Fig.1; $K(T)$ is the same as the superfluid density $\rho_s(T)$ and proportional to $1/\lambda_L^2(T)$. For the temperature dependence of the gaps $\Delta_{h,e}(T)$, we used a phenomenological formula, $\Delta_{h,e}(T) = \Delta_{h,e}(T=0)\tanh(1.74\sqrt{T_c/T-1})$. The values of $\Delta_{h,e}/T_c$ determine the high temperature behavior below T_c. We chose $2\Delta_h/T_c = 3.0$ and $|\Delta_e|/|\Delta_h| = 2.5$ for our calculations.

Figure 2(a) shows the superfluid density $\rho_s(T)$ over $0 < T < T_c$ for different impurity concentrations, $\Gamma/\Delta_e = 0.0, 0.01, 0.04, 0.08$, normalized by $\rho_s^0(T=0)$ of the pure state. We warn the fact that the temperature dependence of $\rho_s(T)$ at high temperatures (say, $0.5 < T/T_c < 1$) does not reflect the low energy DOS nor the impurity effects but it is mainly determined by the temperature dependence of $\Delta_{h,e}(T)$. $\rho_s(T)$ of the pure case ($\Gamma/\Delta_e = 0.0$) shows the exponentially flat temperature dependence at low temperatures, consistent with the fully gapped DOS (see Fig.1(a)) of the $\pm$s-wave state. With increased impurity concentration, $\Gamma/\Delta_e = 0.01$, this full gap behavior still persists. When impurity concentration becomes critical, i.e., $\Gamma/\Delta_e = 0.04$, the DOS become a perfect V-shape down to zero frequency and the exponentially flat region of $\rho_s(T)$ disappears. With further increase of impurity concentration, for $\Gamma/\Delta_e = 0.08$, the DOS is not only a V-shape but it also obtains a finite DOS at zero frequency $N(0) = const.$, and $\rho_s(T)$ becomes even more smooth. To see more clearly the power laws of the low temperature behavior, we plot, in Fig.2(b), the temperature dependent part of the penetration depth $\Delta\lambda(T) = \lambda(T) - \lambda(T=0)$ normalized by $\lambda_0(T=0)$ of the pure state. The power law fittings (black solid lines in Fig.2(b)) clearly confirm that $\Delta\lambda(T) \propto T^3$ at the critical impurity concentration $\Gamma_{imp} = \Gamma_{crit} = 0.04\Delta_e$ and $\Delta\lambda(T) \propto T^2$ for higher concentration $\Gamma_{imp} = 0.08\Delta_e$, as we have shown with an analytic analysis of Eq.(9).

Thermodynamic DOS and transport DOS. – Switching gears, we would like to draw attention to the more general aspect of DOS, which was clearly demonstrated in this paper; namely the fact that *the DOS measured by thermodynamic properties and the DOS measured by transport properties can in general be different*. The DOS of the $\pm$s-wave state with a critical impurity concentration looks a V-shape as shown in Fig.1(a). Here the DOS is the distribution of the quasiparticle energy eigenstates and this distribution can be measured by thermodynamic properties such as specific heat, photoemission, and spin-lattice-relaxation rate $1/T_1$, etc. Therefore, this V-shape DOS is thermodynamically indistinguishable from the V-shape DOS of a pure d-wave SC state. As mentioned, however, angle-resolved-photoemission spectroscopy can still distinguish the presence or absence of the angular (or Fermi surface) anisotropy of the quasiparticle DOS [13–15].

On the other hand, the superfluidity density is a transport quantity defined as

$$\begin{aligned} \vec{J}(r) &= -\frac{c}{4\pi}K(T)\vec{A}(r) = -\frac{c}{4\pi\lambda^2(T)}\vec{A}(r) \\ &= -\frac{e^2}{mc}\rho(T)\vec{A}(r) \end{aligned} \tag{11}$$

in the local limit (London limit). In the non-interacting case (no further quasiparticle scattering after diagonalization of pairing interactions), the BCS theory give a simple formula of the kernel to the vector potential $\vec{A}$ as [37]

$$K(T) = \frac{1}{\lambda_L^2}\Big[1 - 2\int_{\Delta}^{\infty} d\omega\Big(-\frac{\partial f}{\partial\omega}\Big)Re\frac{\omega}{(\omega^2-\Delta^2)^{1/2}}\Big]. \tag{12}$$

The second term is apparently proportional to the thermodynamic DOS $Re\frac{\omega}{(\omega^2-\Delta^2)^{1/2}}$ and when $\tilde{\omega}=\omega+i\eta$ the general expression of the kernel (Eq.(9)) can be converted into Eq.(12). However, once the quasiparticle obtains a finite lifetime due to interactions, Eq.(9) and Eq.(12) can not be interchangeable and we have to use Eq.(9) to calculate the superfluid density and penetration depth. Even for the simplest case of a constant damping $\tilde{\omega}=\omega+i\gamma$, using Eq.(12) would give $\delta\lambda(T)\propto -const.$, but the correct temperature dependence due to a constant damping is $\delta\lambda(T)\propto -\gamma T^2$ as well known in the case of high-Tc cuprates [36] and reproduced in the current paper. When $\tilde{\omega}=\omega+i\beta\omega$, the difference is even more interesting; Eq.(12) predicts $\delta\lambda(T)\propto -\beta T$ but the correct behavior from Eq.(9) produces $\delta\lambda(T)\propto -\beta T^3$. We emphasize that this difference of the DOS depending on the different measurements should be carefully considered for interpretations of various experiments of Fe pnitide SCs.

Conclusion. – We have calculated the superfluid density $\rho_s(T)$ and penetration depth $\lambda(T)$ of the ±s-wave state with impurities of the strong coupling limit. We showed, both by analytic analysis and by numerical calculations, that the temperature dependence of $\rho_s(T)$ and $\lambda(T)$ at low temperatures continuously evolves in a sequence of the forms: exponentially flat $\rightarrow\propto T^3\rightarrow\propto T^2$ with increase of impurity concentration. This result consistently explain the experimental data of *M*-1111 (*M*=Pr, Nd, Sm) [17–19] (flat), (Ba,K)Fe_2As_2 [20] (flat), and Ba(Fe,Co)$_2As_2$ [21,22] ($\propto T^{2-2.5}$). The near $T-$linear behavior of LaFePO [23] data can not be explained by our theory. If the data of LaFePO [23] is indeed confirmed, it indicates that LaFePO may have a different pairing symmetry than the other Fe pnictide SCs. Finally, we noticed that Vorontsov et al. [38], have recently studied the same problem as in this paper, and obtained a similar result $\rho_s(T)\propto T^2$ for high concentration of impurities but obtained a different result $\rho_s(T)\propto T^{1.6}$ for the critical impurity concentration. We think that the origin of this difference mainly arises from the fact that Vorontsov et al. [38] studied a weak coupling impurity scattering and we studied the strong coupling impurity scattering. As a consequence, the definition of the critical impurity concentration and the manner that the SC state becomes gapless with impurities is different in each studies.

* * *

This work was supported by the KOSEF through the Grants No. KRF-2007-521-C00081.

REFERENCES

[1] Y.KAMIHARA ET AL., *J. Am. Chem. Soc.*, **130** (2008) 3296.

[2] G. F. CHEN, Z. LI, D. WU, G. LI, W.Z. HU, J. DONG, P. ZHENG, J.L. LUO, N.L. WANG, *Phys. Rev. Lett.*, **100** (2008) 247002.

[3] X. H. CHEN, T. WU, G. WU, R. LIU, H. CHEN, AND D. FANG, *Nature (London)*, **453** (2008) 761.

[4] Y. WANG, L. SHAN, L. FANG, P. CHENG, C. REN, AND H. WEN, arXiv:0806.1986 (unpublished).

[5] L. SHAN, Y. WANG, X. ZHU, G. MU, L. FANG, C. REN, AND H. WEN, *Europhys. Letters*, **83** (2008) 57004.

[6] T. SATO, S. SOUMA, K. NAKAYAMA, K. TERASHIMA, K. SUGAWARA, T. TAKAHASHI, Y. KAMIHARA, M. HIRANO, H. HOSONO, *J. Phys. Soc. Jpn.*, **77** (2008) 063708.

[7] K. MATANO, Z.A. REN, X.L. DONG, L.L. SUN, Z.X. ZHAO, GUO-QING ZHENG, *Europhys. Lett.*, **83** (2008) 57001.

[8] H.-J. GRAFE, D. PAAR, G. LANG, N. J. CURRO, G. BEHR, J. WERNER, J. HAMANN-BORRERO, C. HESS, N. LEPS, R. KLINGELER, B. BUECHNER, *Phys. Rev. Lett.*, **101** (2008) 047003.

[9] H. MUKUDA, N. TERASAKI, H. KINOUCHI, M. YASHIMA, Y. KITAOKA, S. SUZUKI, S. MIYASAKA, S. TAJIMA, K. MIYAZAWA, P.M. SHIRAGE, H. KITO, H. EISAKI, A. IYO, *J. Phys. Soc. Jpn.*, **77** (2008) 093704.

[10] Y. NAKAI, K. ISHIDA, Y. KAMIHARA, M. HIRANO, AND H. HOSONO, *J. Phys. Soc. Jpn.*, **77** (2008) 073701.

[11] S. KAWASAKI, K. SHIMADA, G. F. CHEN, J. L. LUO, N. L. WANG, AND GUO-QING ZHENG, *Phys. Rev. B*, **78** (2008) 220506.

[12] T. Y. CHEN, Z. TESANOVIC, R. H. LIU, X. H. CHEN, AND C. L. CHIEN, *Nature (London)*, **453** (2008) 1224.

[13] H. DING ET AL., *Euro. Phys. Lett.*, **83** (2008) 47001.

[14] T. KONDO ET AL., *Phys. Rev. Lett.*, **101** (2008) 147003.

[15] L. WRAY, D. QIAN, D. HSIEH, Y. XIA, L. LI, J.G. CHECKELSKY, A. PASUPATHY, K.K. GOMES, A.V. FEDOROV, G.F. CHEN, J.L. LUO, A. YAZDANI, N.P. ONG, N.L. WANG, M.Z. HASAN, arXiv:0808.2185 (unpublished).

[16] G. MU, X. ZHU, L. FANG, L. SHAN, C. REN, AND H. WEN, *Chin. Phys. Lett.*, **25** (2008) 2221.

[17] L. MALONE, J.D. FLETCHER, A. SERAFIN, A. CARRINGTON, N.D. ZHIGADLO, Z. BUKOWSKI, S. KATRYCH, J. KARPINSKI, arXiv:0806.3908 (unpublished).

[18] K. HASHIMOTO, T. SHIBAUCHI, T. KATO, K. IKADA, R. OKAZAKI, H. SHISHIDO, M. ISHIKADO, H. KITO, A. IYO, H. EISAKI, S. SHAMOTO, Y. MATSUDA, *Phys. Rev. Lett.*, **102** (2009) 017002.

[19] C. MARTIN, R. T. GORDON, M. A. TANATAR, M. D. VANNETTE, M. E. TILLMAN, E. D. MUN, P. C. CANFIELD, V. G. KOGAN, G. D. SAMOLYUK, J. SCHMALIAN, R. PROZOROV, arXiv:0807.0876 (unpublished).

[20] K. HASHIMOTO, T. SHIBAUCHI, S. KASAHARA, K. IKADA, T. KATO, R. OKAZAKI, C. J. VAN DER BEEK, M. KONCZYKOWSKI, H. TAKEYA, K. HIRATA, T. TERASHIMA, Y. MATSUDA, arXiv: 0810.3506 (unpublished).

[21] R. T. GORDON, C. MARTIN, H. KIM, N. NI, M. A. TANATAR, J. SCHMALIAN, I. I. MAZIN, S. L. BUD'KO, P. C. CANFIELD, R. PROZOROV, arXiv:0812.3683 (unpublished).

[22] R. PROZOROV, M. A. TANATAR, R. T. GORDON, C. MARTIN, H. KIM, V. G. KOGAN, N. NI, M. E. TILLMAN, S. L. BUD'KO, P. C. CANFIELD, arXiv:0901.3698 (unpublished).

[23] J. D. FLETCHER, A. SERAFIN, L. MALONE, J. ANALYTIS, J-H CHU, A.S. ERICKSON, I.R. FISHER, A. CARRINGTON, arXiv:0812.3858 (unpublished).

[24] I.I. MAZIN, D.J. SINGH, M.D. JOHANNES, M.H. DU, *Phys. Rev. Lett.*, **101** (2008) 057003.

[25] K. KUROKI, S. ONARI, R. ARITA, H. USUI, Y. TANAKA, H. KONTANI, AND H. AOKI , *Phys. Rev. Lett.* , **101** (2008) 087004.

[26] M. M. KORSHUNOV AND I. EREMIN, *Phys. Rev. B*, **78** (2008) 140509.

[27] F. WANG, H. ZHAI, Y. RAN, A. VISHWANATH, DUNG-HAI LEE, *Phys. Rev. Lett.*, **102** (2009) 047005.

[28] Y. BANG AND H.-Y. CHOI, *Phys. Rev. B*, **78** (2008) 134523.
[29] Y. BANG, H.-Y. CHOI, AND H. WON, *Phys. Rev. B*, **79** (2009) 054529.
[30] D. PARKER, O.V. DOLGOV, M.M. KORSHUNOV, A.A. GOLUBOV, I.I. MAZIN , *Phys. Rev. B* , **78** (2008) 134524.
[31] A.V. CHUBUKOV, D.V. EFREMOV, I. EREMIN, *Phys. Rev. B*, **78** (2008) 134512.
[32] M. M. PARISH, J. HU, B. A. BERNEVIG, *Phys. Rev. B*, **78** (2008) 144514.
[33] P. J. HIRSCHFELD, P. WOELFLE, AND D. EINZEL, *Phys. Rev. B* , **37** (1988) 83.
[34] A. V. BALATSKY, I. VEKHTER, AND J.-X. ZHU, *Rev. Mod. Phys.*, **78** (2006) 373, and see more references therein.
[35] Because the integration domain is only over the positive frequencies as $\int_0^\infty d\omega$, we include the ω^3 term whereas the odd power terms are assumed to trivially vanish in the ordinary Sommerfeld expansion.
[36] P.J. HIRSCHFELD AND N. GOLDENFELD, *Phys. Rev. B*, **48** (1993) 4219.
[37] M. TINKHAM, *in Chap. 3, Introduction to superconductivity, 2nd edition* (McGraw-Hill Inc., New York) 1996.
[38] A.B. VORONTSOV, M.G. VAVILOV, A.V. CHUBUKOV, arXiv:0901.0719 (unpublished).